

528.7  
556.04

# A PROPOSED METHOD TO IMPROVE SPRINGTIME AREAL SNOW WATER EQUIVALENT MAPS BY USING SATELLITE IMAGERY

by

RISTO KUITTINEN

Technical Research Centre of Finland

JAAKKO PERÄLÄ

National Board of Waters

## Abstract

The melting of snow is in spring strongly affected by vegetation cover and terrain topography in Finland. By using NOAA imagery it is possible to monitor snowmelt process satisfactorily also in hilly and forested areas. The combination of this snowcover information with snow water equivalent values measured by aerial gamma ray spectrometry gives possibilities to improve the accuracy of areal snow water equivalent estimates during the melting period.

### 1. Background

Since the first meteorological satellites were launched in the early 1960's a lot of research and development work has been carried out for using satellite imagery in snowcover monitoring. Especially in the USA, Canada and the USSR these methods are in the operational stage and used every year (RANGO *et al.*, 1979, BOWLEY *et al.*, 1981, KUPRIANOV, 1983). In this task mainly imagery taken by geostationary and polar-orbiting satellites is used. Visible, near IR and thermal IR parts of the electromagnetic spectrum are used in imaging and mainly visual as well as numerical interpretation is used in determining the snowcovered area.

The main problem of this technique is cloud cover which prevents imagery. However, in most cases the time in which snow is covering the ground is sufficiently long, so that enough cloudless images can be analyzed for determining the snowcover variations. Especially geostationary and polar-orbiting weather satellites give coverage frequent enough for most snowcover monitoring purposes.

At the same time as it became possible to get information on the areal extent of the snowcover by satellite imagery, a technique was developed to measure the water equivalent of the snowcover by gamma-ray spectrometry from aircraft (WMO, 1979).

This technique is now operationally used in Norway, the USA and the USSR and studied in many other countries.

Today it is not possible to obtain areal water equivalents of the snow operationally by satellite imagery (NASA, 1982). One way to get areal values is to combine information obtained by satellite imagery and by gamma-ray techniques. Satellite imagery gives the spatial distribution of the snowcover and gamma-ray technique line and point values of the water equivalent of the snow. This way of combining different kinds of information gives good possibilities to produce quite fast water equivalent value maps for different purposes. Because remote sensing techniques are relatively recent, the measurements made by these techniques are not commonly used in hydrological models. In Switzerland and the USA snowcover data based on remote sensing measurements are used in hydrological models (MARTINEC and RANGO, 1983) and in the USA the possibilities to use remotely sensed data in hydrological models have been studied (PECK *et al.*, 1981, 1982).

## 2. Snowcover monitoring using NOAA imagery

In Finland vegetation cover and land use are locally the most important factors affecting the time of local snowmelt. In mesoscale the amount of snow is also important. In general, snow will melt 10 days earlier in open areas than in forests (SOLANTIE, 1977). Also, topography and elevation of terrain affect the snow melt especially in the northern part of Finland. Figure 1 shows a part of NOAA-7 imagery taken April 26th, 1983. This satellite is a polar-orbiting weather satellite with a multispectral scanner (Advanced Very High Resolution Radiometer, AVHRR), which has 5 channels. Channel 1 operates in the 0.58 to 0.68  $\mu\text{m}$  band and channel 2 in the 0.78 to 1.10  $\mu\text{m}$  band. Due to the unusually warm weather in April, the snow had already melted in southern and central Finland and the snowline went close to a line from Raahe to Joensuu. Figures 2–5 show how the snow was melting in the Kemijärvi–Posio area ( $\lambda = 66^{\circ}30'$ ,  $\varphi = 27^{\circ}30'$ ) from 27th April to 16th May 1983. These figures show clearly how irregular the snowmelt process is

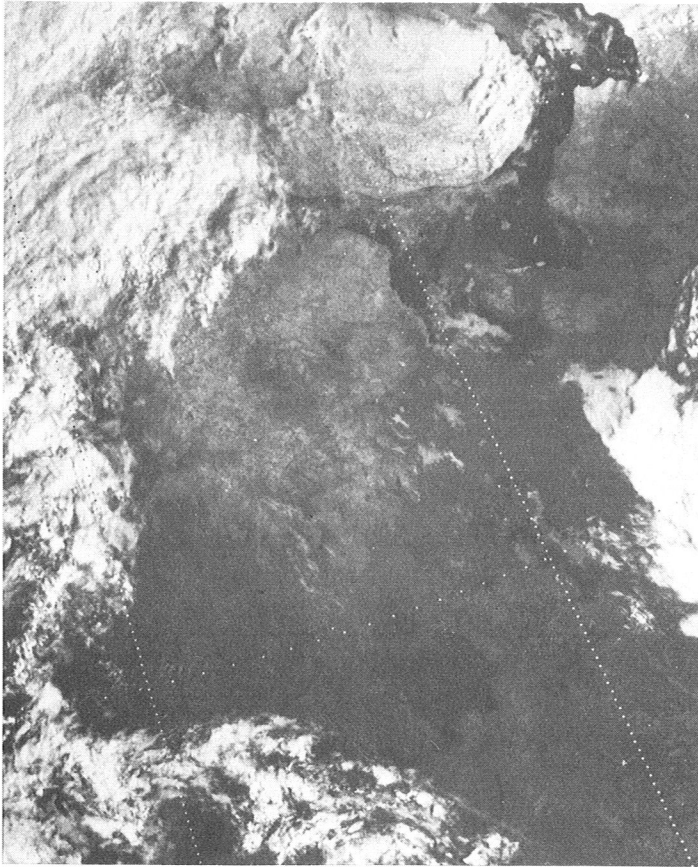


Figure 1. NOAA-7 image taken 26th April, 1983. Snow is in the image darker than clouds which are white.

in this area, and how this kind of data can improve the knowledge of the spatial distribution of the snowcover in the spring.

For studying the effect of land use and type of vegetation cover on the snow-melt process in spring the following classes were interpreted in a NOAA-6 imagery taken 19th August 1980 in the Kemijärvi–Posio area:

1. Water
2. Pine dominated forest
3. Spruce dominated forest

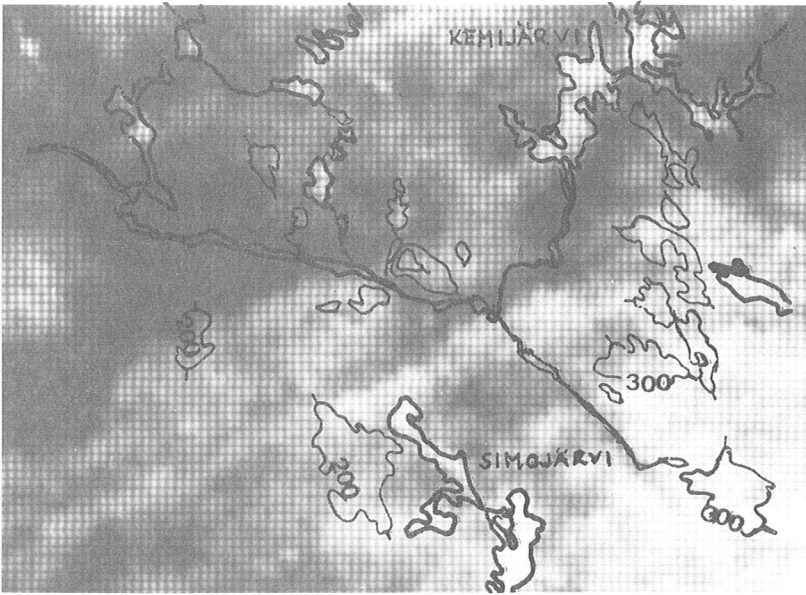


Figure 2. NOAA-7 image taken 27th April, 1983.

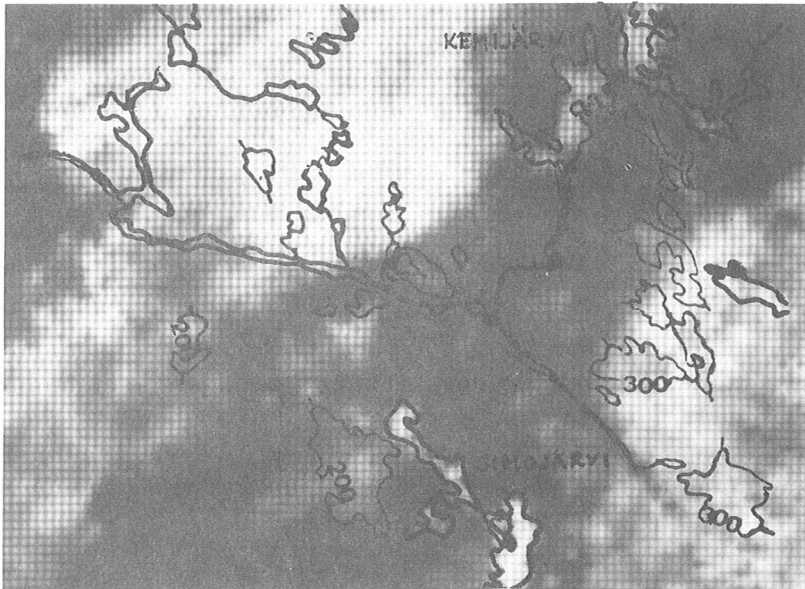


Figure 3. NOAA-7 image taken 3rd May, 1983.

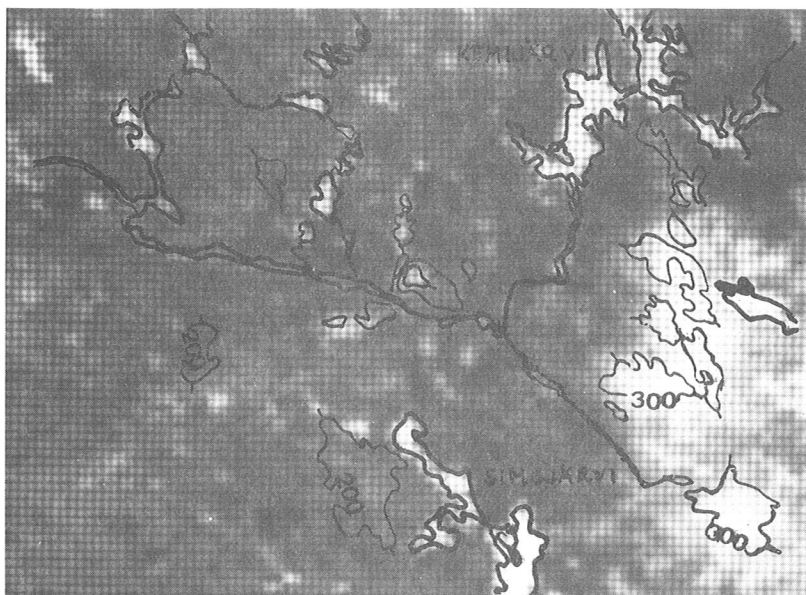


Figure 4. NOAA-7 image taken 9th May, 1983.

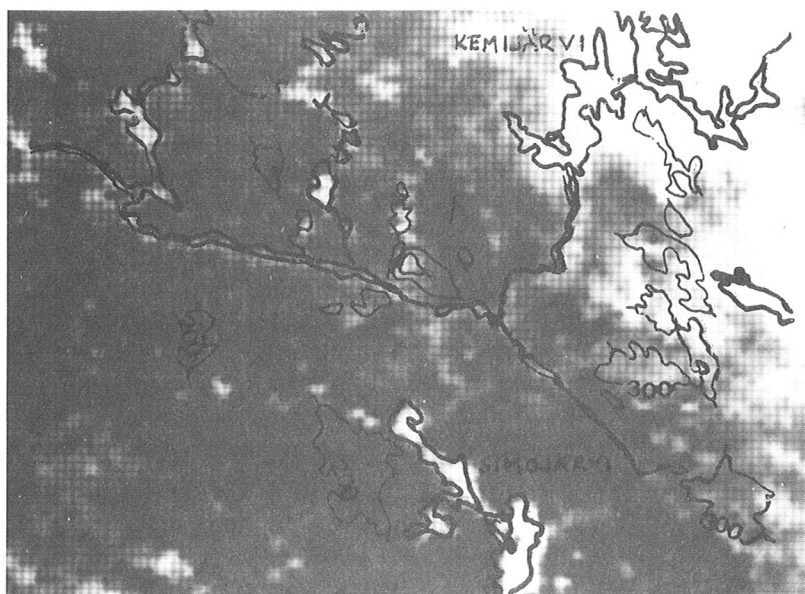


Figure 5. NOAA-7 image taken 16th May, 1983.

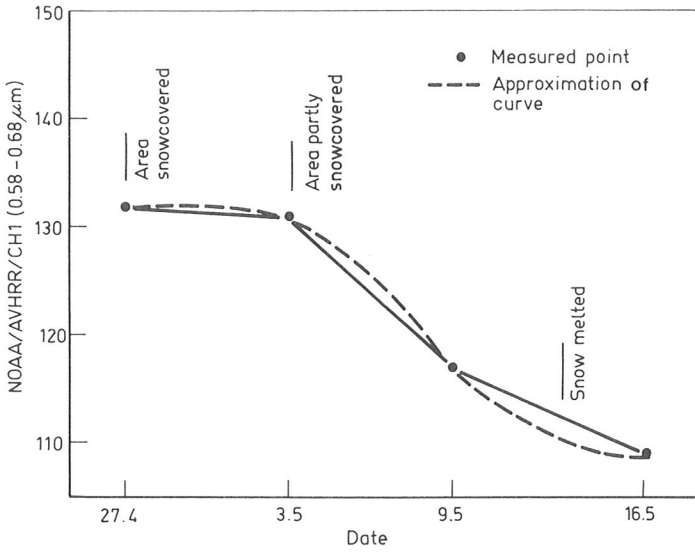


Figure 6. Average radiances of terrain registered by the AVHRR of NOAA satellite during the snowmelt period in 1983.



Figure 7. Snowcovered pine dominated forest.



Figure 8. Melting snow in pine dominated forest.



Figure 9. The last phase of snowmelt in pine dominated forest.

4. Clearcut areas and half open forests }  
 5. Open bogs (including agricultural fields) } Open areas

In the interpretation supervised classification was used.

Figure 6 shows a typical curve which describes how the radiance of a snow-covered area was decreasing during snowmelt when measured by the AVHRR of the NOAA-7 satellite. This curve was noticed to be different for different terrain types and for different elevations. Also aspect has an effect on the shape of this curve. Figure 7 represents the situation in the terrain when the area is snow-covered. Figures 8 and 9 illustrate how the image changes when the snow is melting and only part of the original snowcover is left.

The effect of elevation difference can be noticed in Figures 10 to 12. The snow melts later in the areas located higher up and this can be seen in the curves. Figure 13 shows this phenomenon as seen at ground level. The effect of the vegetation cover on the snowmelt is shown in Figure 14. Snow is melting faster in the open area than in the forest. Seen from ground level the situation is as Figure 15 shows.

The effect of aspect in snowmelt was studied by observing the radiances of the slopes of some large hills measured by the AVHRR channel 1. The ratios of radi-

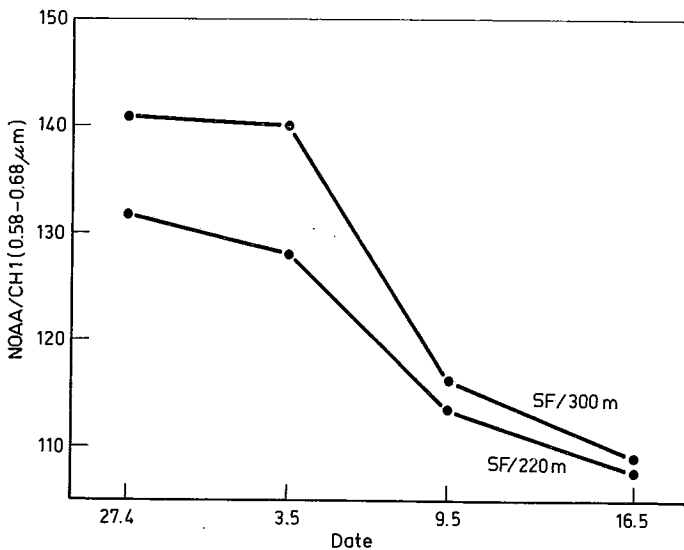


Figure 10. Radiances of spruce dominated forests at the elevations of 220 m and 300 m during the snowmelt period in 1983.



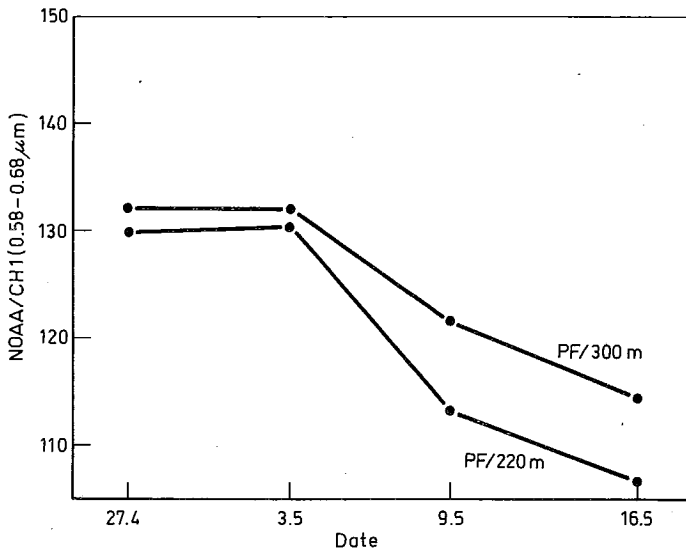


Figure 11. Radiances of pine dominated forests at the elevations of 220 m and 300 m during the snowmelt period in 1983.

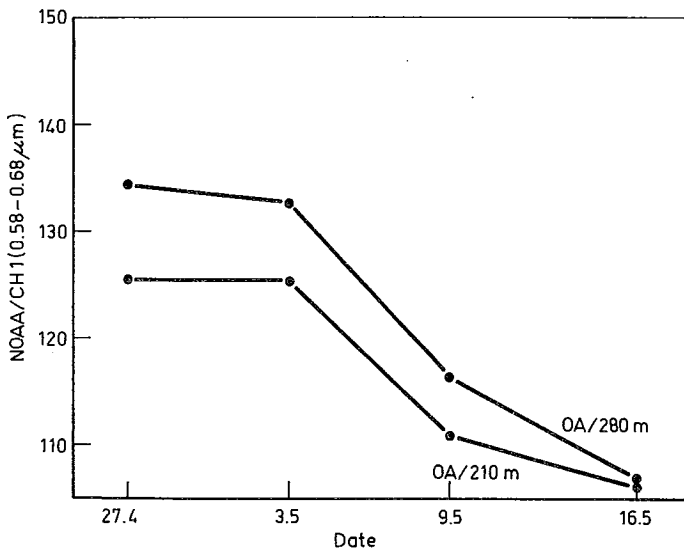


Figure 12. Radiances of open areas at the elevations of 210 m and 280 m during the snowmelt period in 1983.



Figure 13. The hills in the background are covered by snow whereas snow is almost melted in the foreground beneath the hills.

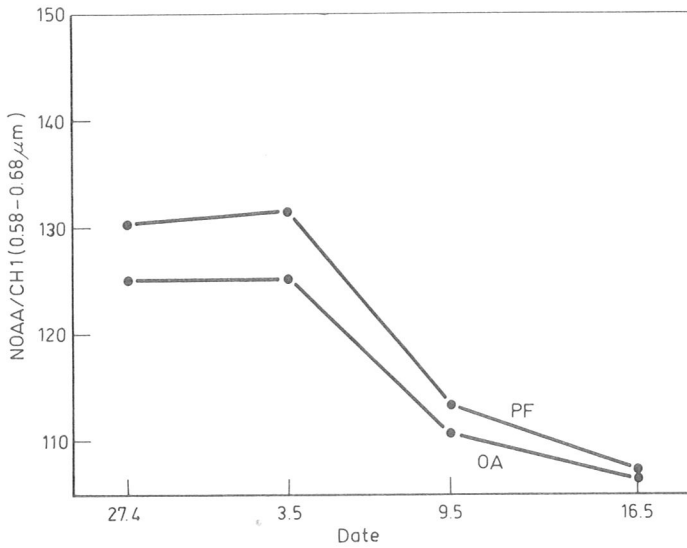


Figure 14. Radiances of open area (OA) and pine dominated forest (PF) at the same elevation 220 m during the snowmelt period in 1983.



Fig. 15. Snow has melted in the bog in the foreground but still exists in the forest.

ation from slopes facing north and slopes facing south were on different dates as presented in the following (pine- and spruce dominated forests):

Date	27.4.	3.5.	1.5.	16.5.
Ratio	1.065	1.014	0.954	0.981

This ratio illustrates the wellknown fact that melting starts on the southern slope. When the ratio is larger than one there are already bare patches in snow on the southern slope. When the ratio is less than one snow has also melted on the northern slope. Because of the warming effect of the radiations measured on the southern slope are higher in early spring. Figures 16 and 17 show the snow in the northern and the southern slope of a hill. In this case the southern slope is almost treeless but the situation is very similar in forested areas.

Figure 18 shows the usefulness of channel 2 of the AVHRR when the time of snowmelt is studied. When all snow has melted and the growing season has not yet begun the radiations measured in this channel are at their lowest. When the growth begins the radiations increase very rapidly because the increasing amount of chlorophyll in nature. Figure 19 shows how the ratios of readings of channels 1 and 2 of the AVHRR are changing when snowmelt is going on in the spring. This also shows that by analyzing NOAA/AVHRR data one can determine when melting is going on and which areas are partly snowless. Also in Figure 19 one can notice



Figure 16. Forest growing on the north slope of a high hill, 3rd May 1983. The snow water equivalent is about 200 mm.



Figure 17. The open south slope of the same hill as in Figure 16. The snow water equivalent is about 50 mm, 3rd May 1983.

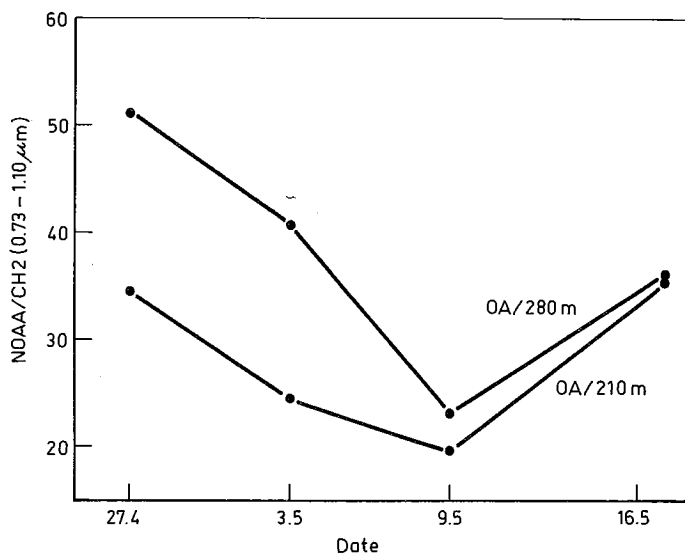


Figure 18. Radiance of open areas at the elevations of 210 m and 280 m during the snowmelt period in 1983.

that variations of observations in the whole image are decreasing towards summer. In this case a part of this variation is caused by clouds which occur in images taken in April and May and the remainder is caused by snowcover. When the standard deviation of the means for test areas were studied, the following results were achieved:

Date	Mean and standard deviation of the standard deviation			
	27.4.	3.5.	9.5.	16.5.
Channel 1	$3.09 \pm 1.98$	$1.42 \pm 0.52$	$1.52 \pm 0.70$	$2.40 \pm 0.76$
Channel 2	$2.37 \pm 1.03$	$1.78 \pm 0.80$	$0.88 \pm 0.60$	$0.89 \pm 0.37$

The image of 16th May (Figure 5) was the most cloudy so that the decreasing effect of the variation of the standard deviation is not quite clear. Later in summer an increase of variation is expected, due to the growth of vegetation.

Although the accumulation of snow is almost the same in microscale in different areas, the melting of snow is strongly affected by vegetation cover and terrain topography, and as can be seen, snowcover can be satisfactorily monitored in spring also in hilly and forested areas when NOAA imagery is used. This gives a possibility to use these images to determine the representativeness of different snowcourses during the melting period.

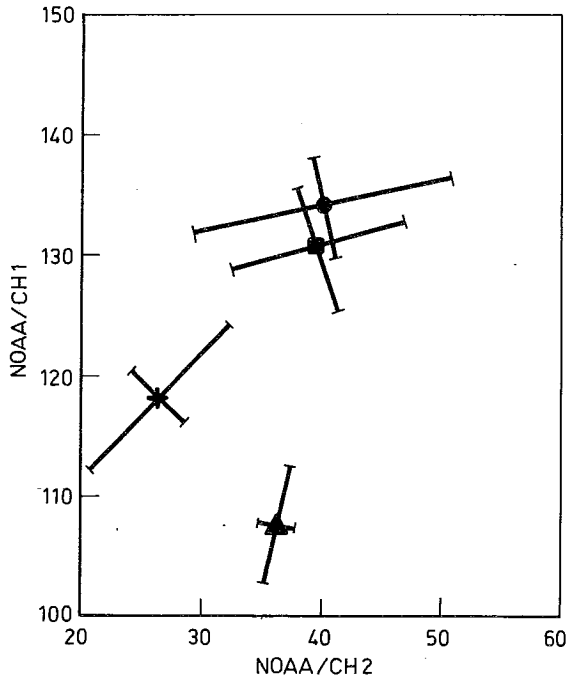


Figure 19. The means and standard deviations of the digital NOAA imageries taken 27th April ■, 3rd May ●, 9th May + and 16th May ▲ in the Kemijärvi–Pori area.

### 3. A method for determining areal water equivalents of snow

Due to the quite frequent cloudiness in spring one can presume that 3 to 5 cloudless NOAA images are available to determine the areal extent of the snow cover during the melting period. At the same period it is possible to carry out 2 to 3 flights for gamma-ray measurements, to determine the water equivalent of the snow. Thus by combining the results of these 5 to 8 measurements it is possible to make reliable maps of the water equivalent of the snow cover for the melting period.

Using summertime NOAA imagery  $X$  and ground truth data the area of interest is classified into classes  $R_i$ . Classification is made using supervised classification, so that

$$X_{ij} \in R_i \text{ if } \begin{cases} a_{ij1} < X_{ij1} < b_{ij1} \\ a_{ij2} < X_{ij2} < b_{ij2} \end{cases},$$

where  $X_{ij}$  is a vector located in the point  $ij$   
 $x_{ijk}$  the  $k$ th element of vector  $X_{ij}$  (channel  $k$ )  
 $a_{ijk}$  and  $b_{ijk}$  are the values which are limiting the area of class  $R_i$  in channel  $k$ .

After classification we have a new image  $Y$ , where each  $Y_{ij}$  is some land use or vegetation type. When this image is added the topographic information, one obtains a new image  $Z$ .

$$Z_{ij} = (t_k, u_l, v_m), \quad k = 1, \dots, o$$

$$l = 1, \dots, p$$

$$m = 1, \dots, q,$$

where  $Z_{ij}$  is a vector located in the point  $i, j$   
 $t$  the land use or vegetation type  
 $u$  the elevation zone  
 $v$  the aspect  
 $k$  the number of different land use and vegetation types ( $1, \dots, o$ )  
 $p$  the number of elevation zones ( $1, \dots, p$ )  
 $m$  the number of aspects ( $1, \dots, q$ ).

When the area of the watershed is divided into equally large squares it is possible to determine for every square the average values of  $Z_{ij}$ 's. At the centre of this square there is a grid point  $G_{ij}$  as follows:

$$G_{ij} = (\bar{t}_k, \bar{u}_l, \bar{v}_m),$$

where  $\bar{t}_k$  is the average of  $t$  in the square  
 $\bar{u}_l$  the average of  $u$  in the square  
 $\bar{v}_m$  the average of  $v$  in the square.

Using a similar interpretation process for every snow course,  $\bar{t}'_k$ 's,  $\bar{u}'_l$ 's and  $\bar{v}'_m$ 's are determined.

On the basis of these basin characteristics information from the whole watershed and the snow courses, the representativeness of every snow course can be determined, within an area, which from earlier snow measurements is known to have, in mesoscale, homogeneous snow accumulation. For this reason the area of a watershed is divided into subareas. Within each subarea the determination of the areal water equivalent  $SWE_{av}$  of the snow cover is made as follows:

- 1) The representativeness of every snow course  $L_i$  for every  $G_{ij}$  is determined on the basis of basin characteristic information.

If  $G_{ij} = (t_2, u_3, v_1)$  and  $L_j = (t_2, u_1, v_1)$

the weight  $P_{ij}$   $L_i$  of the water equivalent of the snow of  $L_i$  at  $G_{ij}$  is determined as follows:

If  $t_{G_{ij}} = t_{L_j}$ ,  $p_t = \frac{1}{3}$  elsewhere 0

If  $u_{G_{ij}} = u_{L_j}$ ,  $p_u = \frac{1}{3}$  elsewhere 0

If  $v_{G_{ij}} = v_{L_j}$ ,  $p_v = \frac{1}{3}$  elsewhere 0

$$P_{ijL_j} = p_t + p_u + p_v,$$

thus the weight  $P_{ijL_j}$  is in this case:

$$P_{ijL_j} = \left( \frac{1}{3} + 0 + \frac{1}{3} \right) = \frac{2}{3}$$

2) For every  $G_{ij}$  we determine the weights  $p_{ij}$  of all snow courses  $L_i$  to that

$$\sum_{k=1}^n p_{ijk} = 1, \text{ where } n \text{ is the number of snow lines in the subarea.}$$

The snow water equivalent  $SWE$  at  $G_{ij}$  is thus

$$SWE = \sum_{k=1}^n p_{ijk} \cdot SW_{L_i}, \text{ where } SW_{L_i} \text{ is the water equivalent.}$$

3) The areal water equivalent of the snow cover  $SWE_{av}$  is

$$SWE_{av} = \frac{1}{r} \sum_{i=1}^r SWE, \text{ where } r \text{ is the number of grid points } G_{ij} \text{ in the subarea.}$$

Before the snow begins to melt during the early stages of the snowmelt NOAA imagery can give very little information of the spatial distribution of the snow-cover because the AVHRR cannot determine the thickness of the snowcover unless it is so thin that bare patches already exist.

#### 4. Discussion

The method described here is now under development. There are still many details which have to be studied more closely, the most important ones are:

- The method which is to be used to determine the average of the basin characteristics for grid points.
- The relationships of snow depletion, between different terrain types during the melting period.



- Radiometric calibration procedures for NOAA data during the snowmelt period.
- The effect of springtime snow accumulation.
- The possibilities to estimate the water equivalent of the snowcover by NOAA imagery during the time, when the snowcover is so thin that bare patches already exist.

For these studies data of several snowmelt periods are needed.

To make the above system operational the following problems must be solved:

- 1) The determination of the water equivalent of the snowcover by gamma-ray techniques must be so fast that the water equivalents determined along snow courses are available within 24 hours after measurements.
- 2) The time needed for processing NOAA data must be about one day. Thus satellite-based snow information would be available on an average within three days after the passage of the satellite.
- 3) The method to compute the areal averages must be stored in a computer so that it may be used instantly and the water equivalent map can be drawn using automatic plotters.

#### REFERENCES

- BOWLEY, C. J., BARNES, J. C. and A. RANGO, 1981: Satellite Snow Mapping and Runoff Prediction Handbook. *NASA Technical Paper 1829*. USA.
- KUPRIANOV, V. V., 1983: *Satellite Information for Surface Water Research*. IAHS Symposium Hydrological Applications of Remote Sensing and Data Transmission. Hamburg, FRG.
- MARTINEC, J. *et al.*, 1983: The Snowmelt – Runoff Model (SRM) User's Manual. *NASA Reference Publication 1100*. USA.
- PECK, E. L. *et al.*, 1981: Review of Hydrologic Models for Evaluating Use of Remote Sensing Capabilities. *NASA-CR-166674*. USA.
- »– , 1981: Strategies for Using Remotely Sensed Data in Hydrologic Models. *NASA-CR-66729*. USA.
- »– , 1982: Combining Remotely Sensed and Other Measurements for Hydrologic Areal Averages. *NASA-CR-170457*. USA.
- Plan of Research for Snowpack Properties Remote Sensing – (PRS)<sup>2</sup>*, 1982. NASA, USA.
- RANGO, A. and R. PETERSON, (Led.), 1979: Operational Applications of Satellite Snowcover Observations. *NASA Conference Publication 2116*. USA.
- SOLANTIE, R., 1977: Lumipeiteajasta Suomesta. On the persistence of snowcover in Finland. *Tutkimusseloste No. 60. Ilmatieteen laitos*. Helsinki.
- Workshop on Remote Sensing of Snow and Soil Moisture by Nuclear Techniques, 1979*. WMO workshop. Voss, Norway.